CHEMISTRY OF MATERIALS

Article

pubs.acs.org/cm

Optimized Thermoelectric Properties of Sb-Doped $Mg_{2(1+z)}Si_{0.5-y}Sn_{0.5}Sb_y$ through Adjustment of the Mg Content

Wei Liu,[†] Xinfeng Tang,*[,†] Han Li,[†] Jeff Sharp,[‡] Xiaoyuan Zhou,[§] and Ctirad Uher[§]

[†]State Key Laboratory of Advanced Technology for Materials Synthesis and Processing, Wuhan University of Technology, Wuhan 430070, China

[‡]Marlow Industries, Inc., 10465 Vista Park Road, Dallas, Texas 75238-1645, United States

[§]Department of Physics, University of Michigan, Ann Arbor, Michigan 48109, United States

Supporting Information

ABSTRACT: $Mg_2Si_{1-x}Sn_x$ compounds are low-cost and environmentally friendly thermoelectric materials expected to be applied as power generators in the intermediate temperature range. Optimization of the thermoelectric properties of $Mg_2Si_{1-x}Sn_x$ compounds can be accomplished by the precise control and adjustment of the Mg content. A series of $Mg_{2(1+z)}Si_{0.5-y}Sn_{0.5}Sb_y$ ($0 \le y \le 0.015$ and $0 \le z \le 0.15$) compounds with controlled Mg content were synthesized by a two-step solid-state reaction method, followed by a spark plasma sintering technique. On the basis of optimized thermoelectric properties via doping with Sb, the effect of a variable content of Mg spanning from understoichiometry to overstoichiometry has been systematically explored. The results indicate that when the actual Mg content exceeds the stoichiometric amount, the dominant point defects in $Mg_{2(1+z)}Si_{0.49}Sn_{0.5}Sb_{0.01}$ compounds are interstitial Mg and Si/Sn vacancies. At the same time, the electron concentration is enhanced with increasing content of Mg. However, when the actual Mg content is substoichiometric, the point defects consist mainly of Mg vacancies that tend to counteract the doping effect of Sb. Thus, the electron concentration of the nominal $Mg_2Si_{0.49}Sn_{0.5}Sb_{0.01}$ compound (in reality a 2 mol % deficiency of Mg) is markedly lower compared with the $Mg_{2.10}Si_{0.49}Sn_{0.5}Sb_{0.01}$ compound, which actually had a 2 mol % excess of Mg. Furthermore, a modest overstoichiometry of Mg enhances the power factor and improves the dimensionless figure of merit. The highest value of $ZT = 1.25$ at 800 K among the compounds was obtained on $Mg_{2.20}Si_{0.49}Sn_{0.5}Sb_{0.01}$, which had an actual Mg excess of 5.5 mol %. The study suggests that point defects, such as interstitial Mg and Si/Sn vacancies, which are created by an overstoichiometric content of Mg, have a positive effect on the electron concentration and thermoelectric properties of n-type $Mg_2Si_{1-x}Sn_x$-based compounds. This research has also established an essential foundation for further optimization of the thermoelectric properties of $Mg_2Si_{1-x}Sn_x$ compounds.

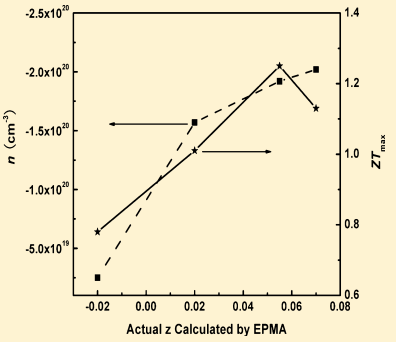

KEYWORDS: *$Mg_{2(1+z)}Si_{0.5-y}Sn_{0.5}Sb_y$, adjustment of the Mg content, point defects, thermoelectric properties*

1. INTRODUCTION

Thermoelectric conversion technology, based on efficient thermoelectric materials, can directly convert waste industrial heat (such as exhaust heat of cars and trucks) into electricity by utilizing the Seebeck effect. This is potentially an important contribution that can assist with relieving the dependence on fossil fuels and helping to mitigate environmental pollution.[1−4] Since the 1990s, Si-based thermoelectric materials, such as Mg_2Si and $MnSi_{1.73}$ compounds, have attracted much attention of the international thermoelectric community because of their obvious advantages of being fabricated from cheap, abundant, and environmentally friendly raw materials, possessing high output power per mass unit, and offering a great prospect for efficient thermoelectric performances.[5−8]

Because of their excellent electrical properties, very low lattice thermal conductivity κ_L, and potentially high dimensionless thermoelectric figure of merit ZT, the study and development of $Mg_2Si_{1-x}Sn_x$ compounds has been a hot topic during the past few years.[6] Currently, the research work on $Mg_2Si_{1-x}Sn_x$ compounds is chiefly focused on optimization of the Sn/Si ratio and on substitutions at the Sn/Si sites so as to enhance the ZT values.[5,9−14] As reported by Zaitsev et al.,[5,6] alloy scattering has the strongest effect on phonons at $x \approx 0.5$ and such compounds have the lowest κ_L, reaching a value of 2 W m^{-1} K^{-1} at room temperature. Doping of such structures that aims at optimizing the electronic transport properties is a promising avenue to achieve high ZT. Such efforts proved fruitful, particularly when doping with Sb, and ZT values in the range of 1.1−1.2 were reported for compounds with $x = 0.4$−0.6.[5,9,10]

According to calculations by Tobola et al.,[15] in $Mg_{2(1-\delta)}Si_{1-x}Sb_x$ compounds, the increasing concentration of Mg vacancies pushes the Fermi level from the band gap ($\delta = 0$) to the valence band ($\delta = 0.1$), and each Mg vacancy creates two

Received: August 17, 2011
Revised: October 16, 2011
Published: November 2, 2011

holes. Experimental results of Nolas et al.[16] and of Dasgupta and co-workers[17] seem to substantiate this viewpoint and indicate that the loss of Mg largely reduces the electron concentration and electrical conductivity of $Mg_{2(1-\delta)}Si_{1-x}Sb_x$ compounds due to the formation of Mg vacancies. Recently, Kato et al.[18] studied the intrinsic point defects in Mg_2Si by density functional theory and found that the Mg content dramatically affects the types and concentration of point defects, along with the thermoelectric properties of Mg_2Si-based compounds. The above team has shown that the loss of Mg is unfavorable to the electrical properties of n-type $Mg_2Si_{1-x}Sn_x$ compounds, while, in contrast, when the content of Mg is slightly larger than or equal to the stoichiometric amount, the electrical transport properties of n-type $Mg_2Si_{1-x}Sn_x$ benefit. While the content of Mg has been shown to influence the transport properties greatly, the precise control and optimization of the amount of Mg remains a challenge to be addressed. On the basis of the thermodynamic principles, the loss of Mg at high temperatures depends directly on the saturated vapor pressure P_e of Mg, given by $\log P_e = -7550/T - 1.41 \log T + 14.915$.[19] P_e of Mg increases exponentially with the temperature from its melting point to its boiling point, resulting in a progressively increasing loss of Mg. As for $Mg_2Si_{1-x}Sn_x$ compounds, while the reaction rate increases with increasing reaction temperature (usually $T \approx 1373$ K in a melting process), because of a large difference in the melting points of the raw materials, the loss of Mg also increases and this is detrimental to precise control of the Mg content. Moreover, Mg is highly reactive and easily reacts with other substances, for example, with O, and this may introduce impurity phases to $Mg_2Si_{1-x}Sn_x$ compounds, something that is highly undesirable.[20,21] Because of the above two major problems related to Mg, we have adjusted the synthesis process in this research. First, we use a two-step solid-state reaction method with a depressed reaction temperature (less than 973 K) so that the loss of Mg can be effectively reduced right from the beginning. As a second step, operations such as the mixing of starting materials and grinding of reaction products are handled in a glovebox to avoid oxidation of Mg and thus minimize the presence of impurity phases. With such precautions, we then proceeded to explore the influences of the Mg content and specifically the beneficial effects of excess Mg content on the thermoelectric properties of Sb-doped $Mg_2Si_{0.5}Sn_{0.5}$ compounds with the aim of optimizing ZT values.

2. EXPERIMENT

$Mg_{2(1+z)}Si_{0.5-y}Sn_{0.5}Sb_y$ ($0 \le y \le 0.015$ and $0 \le z \le 0.15$) compounds were prepared by a two-step solid-state reaction method combined with a subsequent spark plasma sintering (SPS). Commercial high-purity powders of Si (99.99%), Sn (99.9%), and Sb (99.99%) were weighed in stoichiometric quantities, and a powder of Mg was added with an excess of 0−15 mol % over the stoichiometric amount. The raw materials were mixed in an agate mortar in a glovebox, which then were cold-pressed and sealed in quartz tubes in a vacuum for the first-step solid-state reaction with the temperature at 873−973 K. The gained reaction products were powdered in a glovebox, cold-pressed, and sealed under a vacuum, and a second-step solid-state reaction was initiated at 973 K in order to improve the homogeneity and promote the formation of a solid solution. Following the second-step process, the product was ground to a fine powder in a glovebox and then compacted into dense bulk materials using a SPS process at 988 K. The resulting ingots were cut into appropriate sizes for electrical and thermal transport measurements using a diamond disk. The actual Mg content of the final products increased monotonously with the nominal Mg content, implying a controllable Mg content in the adopted synthesis process. Meanwhile, the O content of the final products was about 0.5 mass %, which is slightly more than 0.4 mass % of O measured in the mixture of raw materials. This suggests that the synthesis process used in this work also effectively limits oxidation of Mg, which otherwise results in much greater O gain and represents a serious issue in the preparation of $Mg_2Si_{1-x}Sn_x$ solid solutions.

The structures of the samples were determined using a PANalytical X'Pert Pro type X-ray diffractometer with Cu Kα radiation. The microstructure of the fractured surface and the distribution of the constituent elements of the SPS-compacted samples were characterized by field-emission scanning electron microscopy (SEM) using a Hitachi S-4800 scanning electron microscope. The chemical composition of the resulting samples was analyzed by electron probe microanalysis with the aid of JEOL JXA-8100 equipment. The electrical conductivity and the Seebeck coefficient of the samples were measured simultaneously using a commercial testing instrument (ZEM-1, Ulvac Sinku-Riko) by a standard four-probe method under a He atmosphere. The thermal diffusivity λ was measured by a laser-flash technique on a Netzsch LFA-457 apparatus; the heat capacity C_p at constant pressure was determined using a differential scanning calorimeter on a Q20 device from TA Instruments, and the experimental density d was established by the Archimedes method. All samples showed a very high, near-theoretical density (better than 99%). The thermal conductivity was then calculated using the formula $\kappa = \lambda C_p d$. The temperature range of measurements covered 300−820 K. The Hall effect data were collected using a modified MPMS system from Quantum Design in a field of 1 T. The Hall resistance was monitored with a Linear Research AC Resistance Bridge (LR-700) operated with a 17 Hz excitation frequency. The O content in the samples was ascertained by using a N/O automatic analyzer (LECO TC600) equipped with a standard Fe sample having an O content of 1.09 mass %.

The uncertainty in the values of the electrical conductivity and thermal conductivity was due, in large part, to the uncertainties in the determination of the sample dimensions even though all samples were cut into nominally the same sizes. The overall measurement errors in the electrical conductivity, Seebeck coefficient, and thermal conductivity are estimated as ±5%, ± 3%, and ±5%, respectively.

3. RESULTS AND DISCUSSION

3.1. Exploration of the Best Sb Doping Amount. The influence of Sb doping on the thermoelectric properties of $Mg_{2.20}Si_{0.5-y}Sn_{0.5}Sb_y$ ($0 \le y \le 0.015$) compounds with a fixed excess of 10 mol % of Mg was investigated first. The inset in Figure 1 shows the relationship between the resistivity and

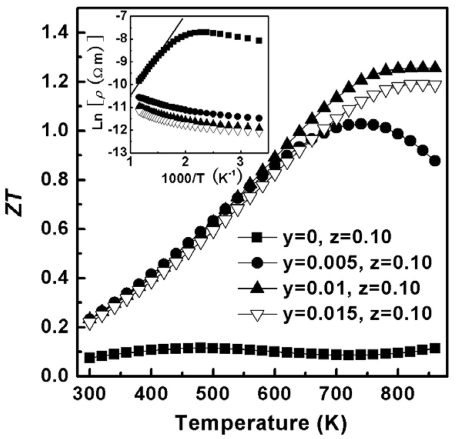

Figure 1. Temperature dependence of ZT values of $Mg_{2.20}Si_{0.5-y}Sn_{0.5}Sb_y$ compounds for a range of Sb doping ($0 \le y \le 0.015$). The inset shows the relationship between the resistivity and temperature for $Mg_{2.20}Si_{0.5-y}Sn_{0.5}Sb_y$.

dx.doi.org/10.1021/cm202445d | Chem. Mater. 2011, 23, 5256−5263

Table 1. Room Temperature Physical Properties of $Mg_{2(1+z)}Si_{0.5-y}Sn_{0.5}Sb_y$ ($0 \le y \le 0.015$ and $0 \le z \le 0.12$) Compounds

nominal composition	actual composition	carrier concentration n (cm^{-3})	carrier mobility μ ($cm^2\ V^{-1}\ s^{-1}$)	reduced Fermi energy $\eta = E_F/k_BT$	estimated effective mass m^*/m_o	Lorenz number L_o ($10^{-8}\ V^2\ K^{-2}$)
$y = 0.01$, $z = 0$	$Mg_{1.96}Si_{0.48}Sn_{0.51}Sb_{0.007}$	2.50×10^{19}	131.25	1.07	0.7	1.73
$y = 0.01$, $z = 0.05$	$Mg_{2.04}Si_{0.52}Sn_{0.47}Sb_{0.0078}$	15.65×10^{19}	46.40575	1.83	1.76	1.84
$y = 0.01$, $z = 0.10$	$Mg_{2.11}Si_{0.52}Sn_{0.48}Sb_{0.0056}$	19.22×10^{19}	47.54162	1.75	2.08	1.83
$y = 0.01$, $z = 0.12$	$Mg_{2.14}Si_{0.49}Sn_{0.50}Sb_{0.0068}$	20.22×10^{19}	55.14342	1.98	1.98	1.84
$y = 0$, $z = 0.10$	$Mg_{2.12}Si_{0.50}Sn_{0.50}$	0.23×10^{19}	84.23913	−2.41	1.01	1.50
$y = 0.005$, $z = 0.10$	$Mg_{2.13}Si_{0.49}Sn_{0.51}Sb_{0.0019}$	10.70×10^{19}	56.19159	1.28	1.69	1.76
$y = 0.015$, $z = 0.10$	$Mg_{2.11}Si_{0.51}Sn_{0.48}Sb_{0.0121}$	23.62×10^{19}	47.52329	2.15	2.07	1.90

temperature for $Mg_{2.20}Si_{0.5-y}Sn_{0.5}Sb_y$ compounds. The results indicate that Sb doping distinctly modifies the electrical conduction of $Mg_{2.20}Si_{0.5-y}Sn_{0.5}Sb_y$: the undoped sample exhibits a typical semiconducting behavior (decreasing resistivity with increasing temperature), while the Sb-doped samples display characteristics of a heavily doped degenerate semiconductor (monotonously increasing resistivity with temperature). The band gap of $E_g \approx 0.58$ eV was determined by fitting the equation $\rho \propto e^{E_g/2k_BT}$ to the data of the undoped sample. This value is a bit smaller than the estimated gap of ~0.65 eV derived from the band gaps of $Mg_2Si_{0.4}Sn_{0.6}$ and $Mg_2Si_{0.6}Sn_{0.4}$.[6] In general, Sb has always been considered as a very effective single-electron donor in Mg_2Si-based materials, resulting in notable enhancements in the electron concentration and electrical conductivity.[5,9−11,15] In the present investigation, a slight amount of Sb doped into the structure increases the electron concentration and electrical conductivity of $Mg_{2.20}Si_{0.5-y}Sn_{0.5}Sb_y$ by 1−2 orders of magnitude; see Table 1 and Figure 2. In turn, this leads to a marked enhancement in

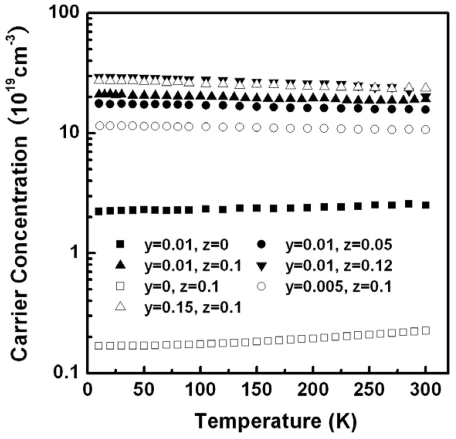

Figure 2. Temperature dependence of the electron concentration (10−300 K) in $Mg_{2(1+z)}Si_{0.5-y}Sn_{0.5}Sb_y$ ($0 \le y \le 0.015$ and $0 \le z \le 0.12$) compounds.

ZT values. For instance, the $Mg_{2.20}Si_{0.49}Sn_{0.5}Sb_{0.01}$ compound with a Sb doping amount of $y = 0.01$ possessed the highest ZT value among all of the samples chiefly because of optimized electrical properties and only partially as a result of decreased κ_L.

3.2. Optimization of the Mg Content. With the Sb doping setting at $y = 0.01$, we then proceeded to establish the optimum content of Mg in $Mg_{2(1+z)}Si_{0.49}Sn_{0.5}Sb_{0.01}$ compounds. The range of Mg excess z covered in this work spans $0 \le z \le 0.15$.

3.2.A. Structural Data. Figure 3 shows X-ray diffraction (XRD) patterns of $Mg_{2(1+z)}Si_{0.49}Sn_{0.5}Sb_{0.01}$ ($0 \le z \le 0.15$)

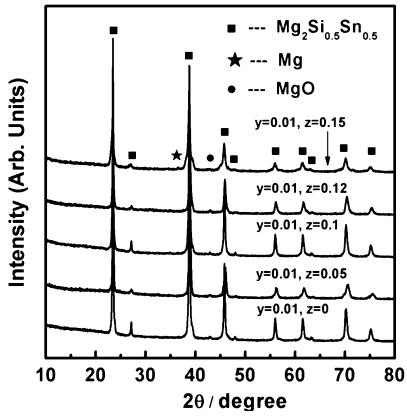

Figure 3. XRD patterns of $Mg_{2(1+z)}Si_{0.49}Sn_{0.5}Sb_{0.01}$ ($0 \le z \le 0.15$) compounds.

compounds. All samples display a series of strong peaks that can be indexed as major peaks of the $Mg_2Si_{0.5}Sn_{0.5}$ solid solution.[22,23] This implies that we indeed obtained samples with the desired structure, as shown in Figure S1 in the Supporting Information. We also find a trace amount of MgO in these materials, which is commonly observed in related works.[10−12,16,17] A weak peak at $2\theta \approx 36.6°$, when $z = 0.15$, was confirmed by differential scanning calorimetry (DSC) analysis (see Figure 4) as that due to Mg. As shown in Figure 4, the

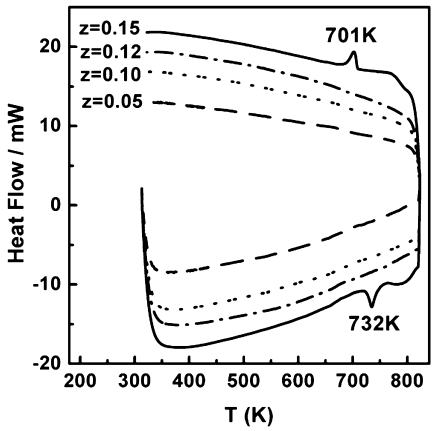

Figure 4. DSC analysis of $Mg_{2(1+z)}Si_{0.49}Sn_{0.5}Sb_{0.01}$ ($0.05 \le z \le 0.15$) compounds in the range of 300−823 K.

sample with $z = 0.15$, but not the samples with $z \le 0.12$, exhibits a reversible reaction with endothermic and exothermic

dx.doi.org/10.1021/cm202445d | Chem. Mater. 2011, 23, 5256−5263

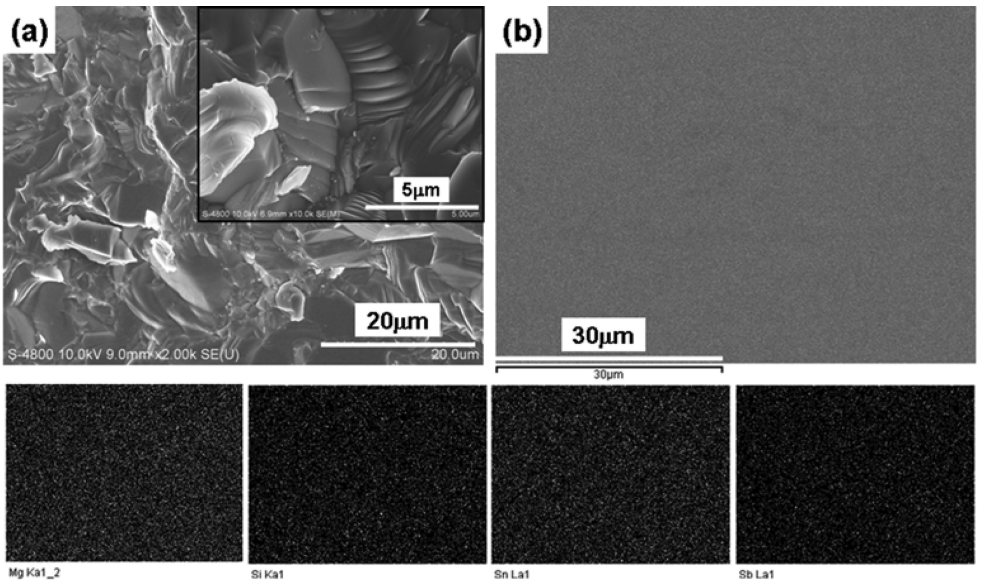

Figure 5. SEM image of the fractured surface (a) and images of the element distribution (b) in the $Mg_{2.20}Si_{0.49}Sn_{0.5}Sb_{0.01}$ compound.

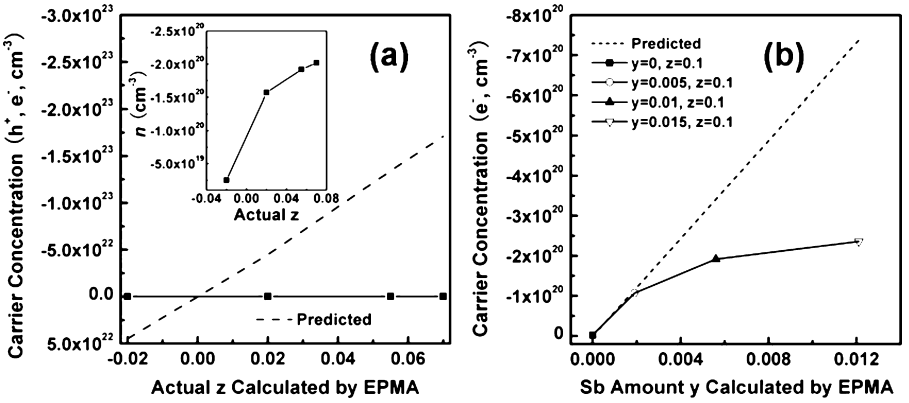

Figure 6. Relationship between the room temperature carrier concentration and the actual Mg excess as well as the Sb amount in $Mg_{2(1+z)}Si_{0.5-y}Sn_{0.5}Sb_y$ ($0 \le y \le 0.015$ and $0 \le z \le 0.12$) compounds. The inset in Figure 5a shows the electron concentration dependence on a finer scale.

peaks at around 715 K. This phenomenon is undisputedly connected with the existing free Mg in the sample with z = 0.15, where a part of free Mg will enter into the crystal lattice at T > 732 K, while precipitation of free Mg occurs when T < 701 K. This result indicates a higher capacity of excess Mg in $Mg_2Si_{0.5}Sn_{0.5}$ at elevated temperatures (T > 732 K) and also reveals the absence of free Mg in the samples with $z \le 0.12$. Thus, while we list the actual compositions of $Mg_{2(1+z)}Si_{0.49}Sn_{0.5}Sb_{0.01}$ in Table 1, it should be understood that single-phase compounds are limited to Mg excess below the nominal z = 0.15. Because the sample with multiphase structures such as the nominal z = 0.15 have degraded electronic properties, we do not consider this compound any further. Figure 5 shows the SEM image of the fractured surface and images of the elemental distribution in the $Mg_{2.20}Si_{0.49}Sn_{0.5}Sb_{0.01}$ compound. In Figure 5a, one notes the grain size that is mainly in the range of 5−20 μm and generally a dense structure of the compounds. The inset in Figure 5a displays inconspicuous and clean grain boundaries without precipitates for $Mg_{2.20}Si_{0.49}Sn_{0.5}Sb_{0.01}$. The distribution of elements in the $Mg_{2.20}Si_{0.49}Sn_{0.5}Sb_{0.01}$ compound is shown in Figure 5b and is typified by good homogeneity on the micrometer scale.

3.2.B. Electrical Transport Properties. Room temperature parameters of $Mg_{2(1+z)}Si_{0.5-y}Sn_{0.5}Sb_y$ ($0 \le y \le 0.015$ and $0 \le z \le 0.12$) compounds are listed in Table 1. Hall measurement data indicate that all $Mg_{2(1+z)}Si_{0.5-y}Sn_{0.5}Sb_y$ samples with different Mg contents and Sb doping amounts exhibit n-type conduction. Within the framework of a simple parabolic-band model, we estimate the electron effective masses m^* from the experimental values of the Seebeck coefficient α and electron concentration n measured at room temperature. The relevant formulas are presented in eqs 1−4.

$$\alpha = \pm \frac{k_B}{e}\left[\frac{(2+r)F_{1+r}(\eta)}{(1+r)F_r(\eta)} - \eta\right] \quad (1)$$

$$n = \frac{4\pi(2k_BTm^*)^{3/2}}{h^3}F_{1/2}(\eta) \quad (2)$$

$$F_i(\eta) = \int_0^\infty \frac{x^i\,dx}{1+\exp(x-\eta)} \quad (3)$$

dx.doi.org/10.1021/cm202445d | *Chem. Mater.* 2011, 23, 5256−5263

$$\eta = E_F/k_BT \quad (4)$$

Here, $F_i(\eta)$ stands for the Fermi integral, η is the reduced Fermi energy, k_B is the Boltzmann constant, h is the Planck constant, r is the scattering factor, and m^* is the effective mass. The value of $r = 0$ was chosen for Mg_2Si-based compounds presuming the dominance of acoustic phonon scattering.[14,24,25]

The formation energy of different kinds of point defects was evaluated by Kato et al.[18] using a first-principles-theory method. The results showed that, for n-type Mg_2Si compounds, the antisite defects Si_{Mg} (an atom of Si located at the Mg sublattice) and Mg vacancies can form readily when the Mg content is less than the stochiometric amount. In contrast, interstitial Mg and Si/Sn vacancies can emerge under the condition of an excess amount of Mg. Thus, the content of Mg affects the electron concentration and electrical properties of n-type Mg_2Si compounds because it gives rise to charged point defects. Moreover, according to the calculations of Tobola et al.,[15] one Mg vacancy represents two holes. Hence, in order to explain the influence of Mg on the electrical properties of $Mg_{2(1+z)}Si_{0.49}Sn_{0.5}Sb_{0.01}$ compounds, we assumed that an excess or loss of Mg will lead to the formation of corresponding quantities of Si/Sn or Mg vacancies, with the former acting as double-electron donors and the latter posing as double-electron acceptors (assuming full ionization). In addition, we presume that one Sb atom substituting on the Si site provides one electron for the conduction band. Although different types of point defects have different effects on the transport properties, the above simple accounting scheme is useful for gauging the overall trend in the charge carrier density. The results are shown as dashed lines in Figure 6. The relationship between the room temperature carrier concentration and the actual excess content of Mg in $Mg_{2(1+z)}Si_{0.49}Sn_{0.5}Sb_{0.01}$ compounds is plotted in Figure 6a, and a finer scale of this dependence is given in the inset of this figure. The electron concentration in $Mg_{2(1+z)}Si_{0.49}Sn_{0.5}Sb_{0.01}$ increases from 2.5×10^{19} to 2.0×10^{20} cm^{-3} when the actual Mg excess z is increased from −2 to +7 mol %. However, the magnitude of the electron concentration still remains some 2−3 orders of magnitude lower than the calculated values. Figure 6b shows the electron concentration as a function of the actual Sb amount, which represents the effectiveness of Sb doping. The data indicate that Sb is fully ionized at low doping levels but its doping efficiency dramatically decreases at higher levels of doping. This suggests one of two things: either the point defects under the condition of overstoichiometry of Mg are dominated not by Si/Sn vacancies but rather by interstitial Mg, which may have a diminished capacity to provide electrons, or the Si/Sn vacancies are electrically inactive in the sense that only a small fraction of them is fully ionized. As already noted, under the conditions of Mg understoichiometry, two types of point defects may exist in $Mg_{2(1+z)}Si_{0.49}Sn_{0.5}Sb_{0.01}$ compounds: antisite defects Si_{Mg} and Mg vacancies, with the former acting as electron donors and the latter playing the role of electron acceptors. Data in Table 1 indicate that a sample with an actual Mg content of $z = -0.02$ has an electron density of only about $^1/_{10}$ of the sample with an actual content of $z = 0.02$. It is thus highly unlikely that antisite defects Si_{Mg} play any role and it is Mg vacancies that suppress the electron density in samples with substoichiometric amounts of Mg. All in all, the type and quantity of point defects in $Mg_2Si_{0.5}Sn_{0.5}$ are largely controlled by the content of Mg, and this, in turn, leads to dramatic differences in the transport behavior of these compounds. Although overstoichiometric contents of Mg certainly seem to benefit the electrical properties of $Mg_2Si_{0.5}Sn_{0.5}$-based compounds, Sb doping appears to be more effective in enhancing the density of the electrons.

The weighted mobility $U = \mu(m^*/m_0)^{3/2}$ is often used to evaluate the optimum electrical properties of thermoelectric semiconductors.[26−28] Our results indicate that the U value improves from 76.9 $cm^2\ V^{-1}\ s^{-1}$ for the sample with nominal z = 0 to 108.3 $cm^2\ V^{-1}\ s^{-1}$ for $z = 0.05$ and then to 142.6 $cm^2\ V^{-1}\ s^{-1}$ at $z = 0.10$, which attests to a remarkable improvement in the electrical properties with increasing content of Mg.

The temperature dependence of the electron concentration (10−300 K) of $Mg_{2(1+z)}Si_{0.5-y}Sn_{0.5}Sb_y$ compounds is plotted in Figure 2. The data indicate that the sample with no Sb doping displays a small increase in the electron concentration with increasing temperature, which is likely caused by excitation of the tail of the electron distribution across the band gap. In contrast, samples doped with Sb all exhibit a nearly temperature-independent trend, suggesting shallow donor levels that are exhausted at relatively low temperatures. The electrical conductivity of $Mg_{2(1+z)}Si_{0.49}Sn_{0.5}Sb_{0.01}$ $(0 \le z \le 0.12)$ compounds as a function of the temperature is shown in Figure 7. The results show that the electrical conductivity in the

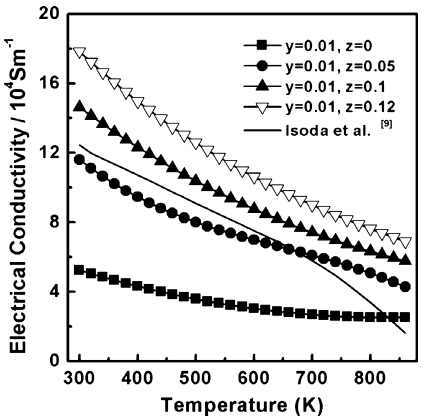

Figure 7. Temperature dependence of the electrical conductivity of $Mg_{2(1+z)}Si_{0.49}Sn_{0.5}Sb_{0.01}$ $(0 \le z \le 0.12)$ compounds.

range of measured temperatures is notably enhanced with increasing z values (increasing excess of Mg), which is mainly the result of markedly increased electron concentration. The electrical conductivity of the $Mg_{2.24}Si_{0.49}Sn_{0.5}Sb_{0.01}$ compound with an actual $z = 0.07$ is improved by 334% at room temperature and 300% at 800 K, compared with the $Mg_2Si_{0.49}Sn_{0.5}Sb_{0.01}$ compound, which has an actual $z = -0.02$. Meanwhile, all $Mg_{2(1+z)}Si_{0.49}Sn_{0.5}Sb_{0.01}$ compounds exhibit a typical heavily doped degenerate semiconductor behavior. The results also reveal that the temperature at which intrinsic excitation of the carriers sets in has moved to higher temperatures with increasing Mg excess amount z. This is particularly apparent with respect to the sample with nominal z = 0 where distinct intrinsic excitations of the carriers commence already near 800 K yet samples with $z > 0$ show no upturns even at 860 K. The solid line in Figure 7 shows the electrical conductivity of the $Mg_{2.10}Si_{0.4925}Sn_{0.5}Sb_{0.0075}$ compound reported by Isoda et al.,[9] which had the electron concentration and electrical conductivity of 1.35×10^{20} cm^{-3} and 13×10^4 S/m, respectively. Similar to our results, the sample had an extrinsic conduction characteristic.

dx.doi.org/10.1021/cm202445d | Chem. Mater. 2011, 23, 5256−5263

Figure 8 displays the temperature dependence of the Seebeck coefficient of $Mg_{2(1+z)}Si_{0.49}Sn_{0.5}Sb_{0.01}$ $(0 \le z \le 0.12)$

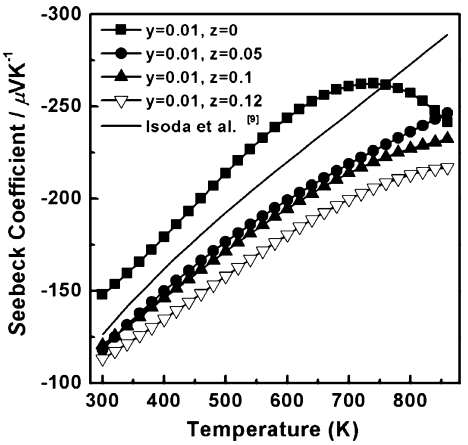

Figure 8. Temperature dependence of the Seebeck coefficient of $Mg_{2(1+z)}Si_{0.49}Sn_{0.5}Sb_{0.01}$ $(0 \le z \le 0.12)$ compounds.

compounds. All samples show negative Seebeck coefficients and, therefore, n-type-dominated conduction in accordance with measurements of the Hall effect. On the whole, the trend in the behavior of the Seebeck coefficient of $Mg_{2(1+z)}Si_{0.49}Sn_{0.5}Sb_{0.01}$ compounds as it relates to temperature and composition is just opposite to the behavior in the electrical conductivity, except for a much lower variance amplitude. The power factor of the compounds was calculated by the equation PF = $\alpha^2\sigma$. Increases in the electrical conductivity with increasing z are much larger than the corresponding reductions in the Seebeck coefficient, and PF is, therefore, considerably enhanced. Compared with the $Mg_2Si_{0.49}Sn_{0.5}Sb_{0.01}$ compound, PF of the $Mg_{2.24}Si_{0.49}Sn_{0.5}Sb_{0.01}$ compound (the nominal z = 0.12) is doubled in the range 300−860 K and attained the largest value of about 3.60×10^{-3} W m^{-1} K^{-2} at 700 K.

3.2.C. Thermal Transport Properties. The total thermal conductivity is written as $\kappa = \kappa_L + \kappa_e + \kappa_B$, where κ_L is the lattice distribution, κ_e stands for the electron distribution, and κ_B represents the bipolar contribution. Figures 9 and 10 show

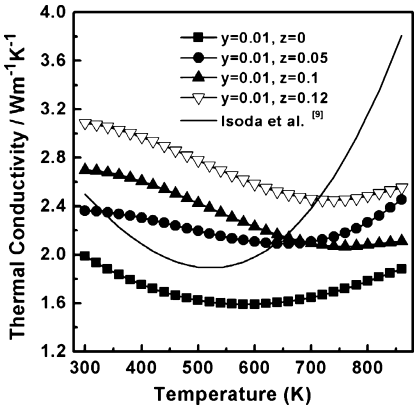

Figure 9. Temperature dependence of the thermal conductivity of $Mg_{2(1+z)}Si_{0.49}Sn_{0.5}Sb_{0.01}$ $(0 \le z \le 0.12)$ compounds.

the temperature dependence of the total thermal conductivity κ and the composite of the lattice thermal conductivity and the bipolar thermal conductivity $\kappa_L + \kappa_B$ of $Mg_{2(1+z)}Si_{0.49}Sn_{0.5}Sb_{0.01}$

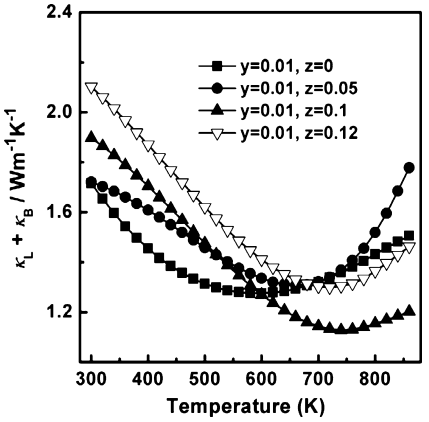

Figure 10. Temperature dependence of the combination of the lattice thermal conductivity and the bipolar thermal conductivity $\kappa_L + \kappa_B$ of the $Mg_{2(1+z)}Si_{0.49}Sn_{0.5}Sb_{0.01}$ $(0 \le z \le 0.12)$ compound.

$(0 \le z \le 0.12)$ compounds. On the basis of the Wiedemann−Franz law, the electronic thermal conductivity κ_e can be estimated from $\kappa_e = L_0\sigma T$, where L_0, σ, and T are the Lorenz number, electrical conductivity, and absolute temperature, respectively. The Lorenz number L_0 can be estimated on the basis of Fermi−Dirac statistics from[24,25]

$$L_0 = \left(\frac{k_B}{e}\right)^2 \left[\frac{3F_0(\eta)\,F_2(\eta) - 4F_1^{\,2}(\eta)}{F_0^{\,2}(\eta)}\right] \quad (5)$$

As shown in Figure 9, κ of $Mg_{2(1+z)}Si_{0.49}Sn_{0.5}Sb_{0.01}$ compounds increases with the z value, which is mainly attributed to large increases in the electronic term κ_e. The solid line in Figure 9 represents the total thermal conductivity of $Mg_{2.10}Si_{0.4925}Sn_{0.5}Sb_{0.0075}$ reported by Isoda et al.[9] In comparison to our sample of similar composition ($Mg_{2.20}Si_{0.49}Sn_{0.5}Sb_{0.01}$), the sample of Isoda et al. shows a rather low κ at low temperatures but very high values at higher temperatures. The values of $\kappa_L + \kappa_B$ of our compounds were calculated and are shown in Figure 10. The combined lattice and bipolar contributions $\kappa_L + \kappa_B$ of $Mg_{2(1+z)}Si_{0.5-y}Sn_{0.5}Sb_y$ compounds show sharp upturns at high temperatures (T > 600 K), which are likely due to a rapidly increasing bipolar contribution as the concentration of minority holes increases upon samples approaching the intrinsic regime of conduction. The lattice thermal conductivity κ_L on its own should be inversely proportional to the temperature as the phonon−phonon umklapp processes are expected to dominate at high temperatures.[25] Because an excess of Mg tends to shift the onset of intrinsic conduction to higher temperatures, it helps to maintain a low $\kappa_L + \kappa_B$ contribution over a broader range of temperatures, and as we shall see shortly, this leads to a shift in the temperature where the highest values of ZT are observed. Moreover, as the excess content of Mg increases, one would expect more intense phonon−point defect scattering that should degrade the lattice thermal conductivity further.[5,6,16,17] According to the experimental data in Figure 10, this is not what is happening. At temperatures below 500 K, with the increasing z value (excess of Mg), the $Mg_{2(1+z)}Si_{0.49}Sn_{0.5}Sb_{0.01}$ compounds display progressively enhanced values of $\kappa_L + \kappa_B$. Because in this (lower) temperature range the bipolar contribution should be minimal, the culprit is the lattice thermal conductivity. Short of postulating that the over-stoichiometric Mg causes major changes to phonon spectra

dx.doi.org/10.1021/cm202445d | Chem. Mater. 2011, 23, 5256−5263

and group velocities or that the estimates of the electronic thermal conductivity, which is the dominant contribution to the overall thermal conductivity for $z > 0$, are unreliable, we do not understand this unexpected behavior.

3.2.D. Dimensionless Figure of Merit ZT and Compatibility Factor s. While Sb doping and Mg nonstoichiometry have a strong effect on the electron concentration and electrical properties of $Mg_{2(1+z)}Si_{0.5-y}Sn_{0.5}Sb_y$, their influence on the lattice thermal conductivity is notably weaker. Therefore, we expect any enhancement in the ZT value of $Mg_{2(1+z)}Si_{0.49}Sn_{0.5}Sb_{0.01}$ to originate mainly from improvements in the electrical properties. This is indeed the case as documented by the plots of the temperature dependence of the dimensionless figure of merit of our compounds in Figure 11. With progressively increasing overstoichiometry of Mg, the figure of merit increases and its peak value shifts to higher temperatures. As we have already noted, this is primarily due to the strongly enhanced electron concentration that arises as a consequence of the increased density of interstitial Mg and Si/Sn vacancies. The highest $ZT = 1.25$ was achieved for the nominal $Mg_{2.20}Si_{0.49}Sn_{0.5}Sb_{0.01}$ compound ($z = 0.1$) at 800 K. This represents about 60% enhancement in comparison to the nominally stoichiometric compound $Mg_2Si_{0.49}Sn_{0.5}Sb_{0.01}$. By repetitive synthesis, we came to a conclusion that $Mg_{2(1+z)}Si_{0.5-y}Sn_{0.5}Sb_y$ compounds can be consistently fabricated with ZT values exceeding 1.10 for a range of electron concentrations between 1.7 and 2.4 × 10^{20} cm^{-3}, which are achieved with $0.0075 \leq y \leq 0.015$ and $z \approx 0.10$. Compared with the results of Isoda et al.,[9] our $Mg_{2.20}Si_{0.49}Sn_{0.5}Sb_{0.01}$ compound has a larger PF and lower thermal conductivity at $T \geq 700$ K and thus reaches higher ZT values.

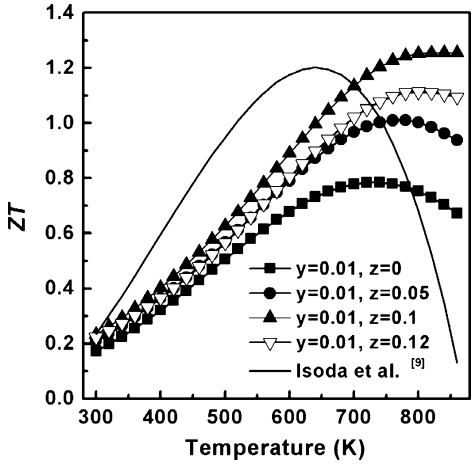

Figure 11. ZT values of $Mg_{2(1+z)}Si_{0.49}Sn_{0.5}Sb_{0.01}$ ($0 \leq z \leq 0.12$) compounds.

In 2003, Snyder and Usell[29] proposed a new physical parameter called the thermoelectric compatibility factor $s = [(1 + ZT)^{1/2} - 1]/\alpha T$ to be used to evaluate whether a given thermoelectric material is suitable for use in segmented couples for power generation applications. The compatibility factor s is a function of the temperature and depends on the Seebeck coefficient. For two different materials to be used in a segmented thermoelectric generator, their compatibility factors should be similar. Figure 12 shows the temperature dependence of the compatibility factor of our $Mg_{2(1+z)}Si_{0.49}Sn_{0.5}Sb_{0.01}$ compounds. The data indicate that the compatibility factor of all our samples changes by less than 50% over the temperature range of measurements, and it is especially flat below 700 K for compounds with high Mg excess. This feature is advantageous for using $Mg_{2(1+z)}Si_{0.49}Sn_{0.5}Sb_{0.01}$ in segmented power generation modules, for instance, in combination with materials such as Bi_2Te_3-based thermoelectrics.

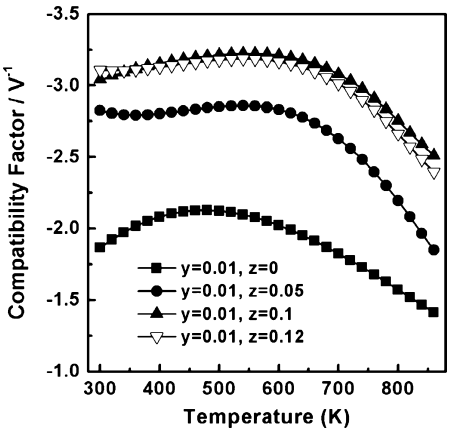

Figure 12. Temperature dependence of the compatibility factor s of $Mg_{2(1+z)}Si_{0.49}Sn_{0.5}Sb_{0.01}$ ($0 \leq z \leq 0.12$) compounds.

4. CONCLUSION

In this work, we studied $Mg_2Si_{0.5}Sn_{0.5}$-based compounds that feature a suitable band gap (~0.5 eV), a controllable carrier (electron) concentration in the range of 10^{18}–3 × 10^{20} cm^{-3}, and a low lattice thermal conductivity. Optimizing the doping amount of Sb at $y = 0.01$, we studied the influence of Mg nonstoichiometry on the electrical and thermal transport properties of $Mg_{2(1+z)}Si_{0.49}Sn_{0.5}Sb_{0.01}$ compounds for a range of z values.

The results indicate that whenever the actual Mg content is overstoichiometric, point defects in $Mg_{2(1+z)}Si_{0.49}Sn_{0.5}Sb_{0.01}$ compounds comprise mainly interstitial Mg and Si/Sn vacancies that both contribute to dramatic enhancements in the concentration of electrons. In contrast, substoichiometric amounts of Mg give rise to Mg vacancies that counteract the effect of Sb doping and suppress the electron concentration. Overstoichiometry of Mg thus leads to a strong enhancement in the electrical conductivity that weighs over suppression of the Seebeck coefficient and results in notably enhanced power factors. Compared with the nominally stoichiometric $Mg_2Si_{0.49}Sn_{0.5}Sb_{0.01}$, the room temperature electron concentration and PF of $Mg_{2.24}Si_{0.49}Sn_{0.5}Sb_{0.01}$ has improved by 1 order of magnitude and a factor of 2, respectively. Somewhat surprisingly, Mg overstoichiometry has an opposite effect on the lattice thermal conductivity from what one would expect for a system with a greater density of point defects, namely, the lattice thermal conductivity seems to increase with the increasing excess of Mg, at least in the temperature range below 500 K. We do not have a good explanation for this at this time. Nevertheless, the remarkable enhancement of the electrical conductivity with the rising excess of Mg results in significant improvements in the figure of merit, which reaches values better than 1.2 at 800 K for a compound with a nominal Mg excess of $z = 0.1$. We have also shown by repeated synthesis and measurements that one can consistently prepare these compounds with a figure of merit better than 1.1 for a wide range of Si/Sn substitutions provided the Mg excess is near $z = 0.1$. Although we can also effectively control the electron

dx.doi.org/10.1021/cm202445d | Chem. Mater. 2011, 23, 5256–5263

concentration through further increases in the level of Sb doping while decreasing the degree of overstoichiometry of Mg, some overstoichiometry of Mg is needed to maintain an optimal electron concentration in $Mg_{2(1+z)}Si_{0.5-y}Sn_{0.5}Sb_y$ because at high doping levels Sb has a significantly reduced ability to supply electrons to the conduction band. The work has shown that overstoichiometry of Mg is an important element in preparing high-performance n-type thermoelectric materials based on the $Mg_2Si_{1-x}Sn_x$ compounds.

■ ASSOCIATED CONTENT

Ⓢ Supporting Information

XRD spectra of $Mg_2Si_{1-x}Sn_x$ compounds and temperature cycling test of the thermoelectric properties for $Mg_{2.20}Si_{0.49}Sn_{0.5}Sb_{0.01}$ compound. This material is available free of charge via the Internet at http://pubs.acs.org.

■ AUTHOR INFORMATION

Corresponding Author

*E-mail: tangxf@whut.edu.cn.

■ ACKNOWLEDGMENTS

We acknowledge support of the National Basic Research Program of China (Grants 2007CB607501 and 2007CB607503), the Natural Science Foundation of China (Grants 50672118, 50731006, and 51002112), the 111 Project (Grant B07040), the Fundamental Research Funds for the Central Universities (Grant 2010-IV-046), the International Science & Technology Cooperation Program of China (Grant 2011DFB60150), and the CERC−CVC U.S.−China program supported by the U.S. Department of Energy, along with support from Marlow Industries, Inc.

■ REFERENCES

(1) Ioffe, A. F. *Semiconductor Thermoelements and Thermoelectric Cooling*; Infosearch: London, 1957.
(2) Nolas, G. H.; Sharp, G. J.; Goldsmid, H. J. *Thermoelectrics*; Springer: Berlin, 2001.
(3) Matsubara, K. Proceedings of the 21th International Conference on Thermoelectrics, Piscataway, NJ, 2002; IEEE Catalog No. 02TH8657; p 418.
(4) Crane, D. T.; Lagrandeur, J. W. *J. Electron. Mater.* **2010**, *39*, 2142.
(5) Zaitsev, V. K.; Fedorov, M. I.; Gurieva, E. A.; Eremin, I. S.; Konstantinov, P. P.; Samunin, Y. A.; Vedernikov, M. V. *Phys. Rev. B* **2006**, *74*, 045207.
(6) Zaitsev, V. K.; Fedorov, M. I.; Eremin, I. S.; Gurieva, E. A. In *Thermoelectric Handbook, Macro to Nano*; Rowe, D. M., Ed.; CRC Taylor & Francis: Oxon, U.K., 2006; Chapters 29 and 31.
(7) Kishida, K.; Ishida, A.; Koyama, T.; Harada, S.; Okamoto, N. L.; Tanaka, K.; Inui, H. *Acta Mater.* **2009**, *57*, 2010.
(8) Luo, W. H.; Li, H.; Yan, Y. G.; Lin, Z. B.; Tang, X. F.; Zhang, Q. J.; Uher, C. *Intermetallics* **2011**, *19*, 404.
(9) Isoda, Y.; Nagai, T.; Fujiu, H.; Imai, Y.; Shinohara, Y. Proceedings of the 25th International Conference on Thermoelectrics, Vienna, Austria, 2006; IEEE Catalog No. 06TH8931; p 406.
(10) Zhang, Q.; He, J.; Zhu, T. J.; Zhang, S. N.; Zhao, X. B.; Tritt, T. M. *Appl. Phys. Lett.* **2008**, *93*, 102109.
(11) Liu, W.; Tang, X. F.; Sharp, J. *J. Phys. D: Appl. Phys.* **2010**, *43*, 085406.
(12) Zhang, Q.; He, J.; Zhao, X. B.; Zhang, S. N.; Zhu, T. J.; Yin, H.; Tritt, T. M. *J. Phys. D: Appl. Phys.* **2008**, *41*, 185103.
(13) Gao, H. L.; Zhu, T. J.; Liu, X. X.; Chen, L. X.; Zhao, X. B. *J. Mater. Chem.* **2011**, DOI: 10.1039/c1jmooo25j.
(14) Zhang, Q.; Yin, H; Zhao, X. B.; He, J.; Ji, X. H.; Zhu, T. J.; Tritt, T. M. *Phys. Status Solidi A* **2008**, *205*, 1657.
(15) Tobola, J.; Kaprzyk, S.; Scherrer, H. *J. Electron Mater.* DOI: 10.1007/s11664-009-1000-3.
(16) Nolas, G. S.; Wang, D.; Beekman, M. *Phys. Rev. B* **2007**, *76*, 235204.
(17) Dasgupta, T.; Stiewe, C.; Zhou, A. J.; Boettcher, L.; Mueller, E. *Phys. Rev. B* **2011**, *83*, 235207.
(18) Kato, A.; Yagi, T.; Fukusako, N. *J. Phys.: Condens. Matter* **2009**, *21*, 205801.
(19) Kubaschewski, O.; Evans, E. *Metallurgical Thermochemistry [M]*, 3rd ed.; Pergamon Press: London, 1958.
(20) Jung, I. H.; Kang, D.-H.; Park, W. J.; Kim, N. J.; Ahn, S. H. *CALPHAD* **2007**, *31*, 192.
(21) Yo Shinaga, M.; Iida, T.; Noda, M.; Endo, T.; Takanashi, Y. *Thin Solid Films* **2004**, *461*, 86.
(22) Luo, W. J.; Yang, M. J.; Chen, F.; Shen, Q.; Jiang, H. Y.; Zhang, L. M. *Mater. Sci. Eng. B* **2009**, *157*, 96.
(23) Zhang, Q.; Zhu, T. J.; Zhou, A. J.; Yin, H.; Zhao, X. B. *Phys. Scr.* **2007**, *T129*, 123.
(24) Noda, Y.; Kon, H.; Furukawa, Y.; Otsuka, N.; Nishida, I. A.; Masumoto, K. *Mater. Trans., JIM* **1992**, *33*, 845.
(25) Isoda, Y.; Nagai, T.; Fujiu, H.; Imai, Y.; Shinohara, Y. Proceedings of the 26th International Conference on Thermoelectrics, Jeju Island, South Korea, 2007; IEEE Catalog No. CFP07404; p 251.
(26) Mahan, G. D. In *Solid State Physics*; Ehrenreich, H., Spaepen, F., Eds.; Academic Press: New York, 1998; Vol. *51*, p 81.
(27) Goldsmid, H. J. *Thermoelectric Refrigerator*; Plenum: New York, 1964.
(28) Slack, G. A. In *CRC Handbook of Thermoelectrics*; Rowe, D. M., Ed.;CRC Press: Boca Raton, FL, 1995; Chapter 34.
(29) Snyder, G. J.; Ursell, T. S. *Phys. Rev. Lett.* **2003**, *91*, 148301.